AIMS Materials Science, 6(4): 464–483.
DOI: 10.3934/matersci.2019.4.464
Received: 14 April 2019
Accepted: 04 June 2019
Published: 11 June 2019

http://www.aimspress.com/journal/Materials

Research article

Optimum molar ratio of H_2 and H_2O to reduce CO_2 using Pd/TiO_2

Akira Nishimura[1,*], Tadaki Inoue[1], Yoshito Sakakibara[1], Masafumi Hirota[1], Akira Koshio[2], Fumio Kokai[2] and Eric Hu[3]

[1] Division of Mechanical Engineering, Graduate School of Engineering, Mie University, Tsu, Mie, 514-8507, JAPAN
[2] Division of Chemistry for Materials, Graduate School of Engineering, Mie University, Tsu, Mie, 514-8507, JAPAN
[3] School of Mechanical Engineering, the University of Adelaide, Australia

*** Correspondence:** Email: nisimura@mach.mie-u.ac.jp; Tel: +81592319747; Fax: +81592319747.

Abstract: This study investigated the optimum moral ratio of CO_2 and reductants H_2O and H_2 to obtain high CO_2 reduction performance of Pd/TiO_2 photocatalyst. The Pd/TiO_2 film photocatalyst is prepared by sol-gel and dip-coating process to form TiO_2 film and by pulse arc plasma method to dope Pd. The prepared Pd/TiO_2 film was characterized by SEM, EPMA and EELS. The impact of overlapping two Pd/TiO_2 films on CO_2 reduction performance was also investigated to utilize the light and prepared photocatalyst more effectively. Moreover, this study investigated the characteristics of Pd/TiO_2 film to reduce CO_2 under the illumination condition of Xe lamp with or without ultraviolet (UV) light. It is found when the moral ratio of $CO_2/H_2/H_2O$ is set at 1:0.5:0.5, the best CO_2 reduction performance has been obtained under the illumination conditions of Xe lamp with and without UV light. It is revealed that the moral quantity of CH_4 per weight of photocatalyst for overlapped Pd/TiO_2 film is 8.14 μmol/g for the moral ratio of $CO_2/H_2/H_2O$ of 1:0.5:0.5 under the illumination condition of Xe lamp with UV light, which is approximately 1.1 times larger than that for one Pd/TiO_2 film. It can be concluded that the optimum moral ratio of $CO_2/H_2/H_2O$, for the CO_2 reduction reaction, is 1:0.5:0.5.

Keywords: Pd/TiO_2 photocatalyst; CO_2 reduction; overlapping effect; reductant

1. Introduction

Due to the increase in the global mean concentration of CO_2 up to 407.8 ppmV as at February in

2019 [1], new CO_2 utilization technology to reduce the amount of CO_2 is required.

This study focuses on CO_2 reduction and conversion into fuel by photocatalysis. TiO_2 is the most common photocatalyt since it is convenient, inexpensive and has strong durability for chemicals and corrosion [2]. TiO_2 is popular photocatalyst that can reduce CO_2 into CO, CH_4, CH_3OH, and H_2 etc. with ultraviolet (UV) light [3–5].

Unfortunately, pure TiO_2 can only be activated under UV light illumination, it is not very effective under sunlight illumination as UV light accounts for only approximately 4% in the solar spectrum. In addition, the rate of electron/hole pair recombination is faster than the rate of chemical interaction between the adsorbents during redox reactions when using TiO_2 [6].

According to recent research [3], many trials have been conducted for TiO_2 to promote the performance of absorbing a photon with visible light illumination as well as to reduce the electron-hole recombination rate. For example, the previous studies investigated doping precious metal such as Pt [7], Ag [8], Au [9], Cu [10,11], composite material formed by GaP and TiO_2 [12], complex assembly CdS/TiO_2 to utilize two photocatalysts that have different band gaps [13], carbon-based AgBr nanocomposites TiO_2 [14], $CuInS_2$ sensitized TiO_2 hybrid nanofibers [15] and preparation procedure of TiO_2 using two alcohols (ethanol and isopropyl alcohol) and supercritical CO_2 [16] to promote the performance of TiO_2. Though the CO_2 reduction performance was improved by these trials, the concentrations of the products were still low, which was ranging from 1 to 150 μmol/g-cat [7–16].

Among various metals have been used for doping, Pt is reportedly a good dopant for TiO_2 [17–19]. However, Pd is considered as a favorite candidate [20–22], as Pd can extend the absorption band to 400–800 nm [23,24], which covers the whole visible light range. Pd/TiO_2 performs a higher reduction performance compared to pure TiO_2, especially, to produce hydrocarbon [23–25].

According to the literature survey, H_2O or H_2 was normally used as the reductant for CO_2 reduction over Pd/TiO_2 [20–26]. In studies of CO_2 reducing with H_2O [20–25], the mixture ratio of CO_2 and H_2O was fixed, but the ratio was not controlled and unclear. According to the report on CO_2 reduction with H_2 [26], the moral ratio of CO_2:H_2 was fixed at 1:4, but the impact of the ratio on CO_2 reduction performance of Pd/TiO_2 was not investigated. Though it is thought that the mixture ratio of CO_2 and reductants influences the CO_2 reduction performance of Pd/TiO_2, there was no study investigating it. In addition, the effect of combination of H_2O and H_2 as reductant on CO_2 reduction over Pd/TiO_2 was not investigated yet.

To promote the CO_2 reduction performance, the optimum reductant providing the proton (H^+) should be clarified. According to the previous studies [27–30], the reaction mechanism to reduce CO_2 with H_2O can be summarized as shown below:

<Photocatalytic reaction>

$$TiO_2 + h\nu \rightarrow h^+ + e^- \quad (1)$$

<Oxidization>

$$2H_2O + 4h^+ \rightarrow 4H^+ + O_2 \quad (2)$$

<Reduction>

$$CO_2 + 2H^+ + 2e^- \rightarrow CO + H_2O \quad (3)$$

$$CO_2 + 8H^+ + 8e^- \rightarrow CH_4 + 2H_2O \quad (4)$$

The reaction mechanism to reduce CO_2 with H_2 can be summarized as shown below [31].

<Photocatalytic reaction>

$$TiO_2 + h\nu \rightarrow h^+ + e^- \quad (5)$$

<Oxidization>

$$H_2 \rightarrow 2H^+ + 2e^- \quad (6)$$

<Reduction>

$$CO_2 + e^- \rightarrow \bullet CO_2^- \quad (7)$$

$$\bullet CO_2^- + H^+ + e^- \rightarrow HCOO^- \quad (8)$$

$$HCOO^- + H^+ \rightarrow CO + H_2O \quad (9)$$

$$H^+ + e^- \rightarrow \bullet H \quad (10)$$

$$CO_2 + 8e^- + 8\bullet H \rightarrow CH_4 + 2H_2O \quad (11)$$

Though a few studies using pure TiO_2 under $CO_2/H_2/H_2O$ condition were reported [31–33], the effect of ratio of CO_2, H_2 and H_2O as well as the effect of Pd doping with TiO_2 on CO_2 reduction characteristics was not investigated previously.

Consequently, the purpose of this study was to clarify the effect of moral ratio of CO_2 and reductants of H_2 and H_2O on CO_2 reduction characteristics of Pd/TiO_2. Additionally, the present study also aims to clarify the optimum combination of reductants.

In the present paper, TiO_2 film is coated on netlike glass fiber (SILIGLASS U, Nihonmuki Co.) by sol-gel and dip-coating process. Glass fiber whose diameter is about 10 μm is weaved as a net, resulting in the diameter of collected fiber of approximately 1 mm. As to the specification of each fiber, the porous diameter is approximately 1 nm and the specific surface area is approximately 400 m^2/g. The composition of netlike glass fiber is SiO_2 of 96 wt%. The aperture area is approximately 2 mm × 2 mm. Due to the porous structure of the netlike glass fiber, TiO_2 film can be captured on netlike glass fiber easily in the step of preparation by sol-gel and dip-coating procedure. Additionally, it was believed that CO_2 would be more easily absorbed by the prepared photocatalyst since the fiber has the porous characteristics.

After the coating of TiO_2, this study loads nanosized Pd particles on TiO_2 by pulse arc plasma method applying high voltage. The pulse number can control the quantity of Pd loaded on TiO_2. We set the pulse number at 100 [34].

Since the netlike glass fiber is transparent, the light can pass through the netlike glass fiber. The present study has also investigated if two Pd/TiO_2 coated netlike glass fiber discs were put one on top of the other (with certain distance, i.e., overlapping), what impact/improvement would be on the CO_2 reduction performance. The following merits were expected by overlapping: (1) effective light utilization, (2) increment of usable photocatalyst to reduce CO_2.

In this paper, the characterization of Pd/TiO_2 was conducted by Scanning Electron Microscope (SEM), Electron Probe Micro Analyzer (EPMA), Scanning Transmission Electron Microscope (STEM), Energy Dispersive X-ray Spectrometer (EDS) and Electron Energy Loss Spectrum (EELS) analysis before CO_2 reduction experiment. This study investigated the performance of CO_2 reduction with H_2 and H_2O with illumination of Xe lamp including or excluding UV light. The combination of

$CO_2/H_2/H_2O$ was changed for 1:0.5:0.5, 1:0.5:1, 1:1:0.5, 1:1:1, 1:2:2 based on moral ratio to clarify the optimum combination of $CO_2/H_2/H_2O$ for CO_2 reduction with Pd/TiO_2. In addition, the effect of overlapping two layers of Pd/TiO_2 coated netlike glass fiber on CO_2 reduction performance was investigated.

2. Materials and method

2.1. Procedure of Pd/TiO_2 photocatalyst preparation

This study prepared TiO_2 film using sol-gel and dip-coating procedure [34–36]. At first, $[(CH_3)_2CHO]_4Ti$ (95 wt% purification, produced by Nacalai Tesque Co.) of 0.3 mol, anhydrous C_2H_5OH (99.5 wt% purification, produced by Nacalai Tesque Co.) of 2.4 mol, distilled water of 0.3 mol, and HCl (35 wt% purification, produced by Nacalai Tesque Co.) of 0.07 mol were mixed to make TiO_2 sol solution. As the basis to coat TiO_2 film, this study cut off the sheet of netlike glass fiber as disc shape whose diameter and thickness were 50 mm and 1 mm, respectively. After that, this study immersed the disc shaped netlike glass fiber into TiO_2 sol solution at 1.5 mm/s and lifted at 0.22 mm/s. In the next step, we dried it out and heated up controlling firing temperature (*FT*) and firing duration time (*FD*), where this study set *FT* and *FD* at 623 K and 180 s, respectively. Therefore, TiO_2 film was coated on netlike glass disc. Pulse arc plasma method was selected to load Pd on TiO_2 film. This study applied the pulse arc plasma gun device (ARL-300, produced by ULVAC, Inc.) with Pd electrode having diameter of 10 mm. This study set TiO_2 film coated on netlike glass fiber in the vacuumed chamber of the pulse arc plasma gun device. After that, Pd electrode emitted nanosized Pd particles under the condition of the voltage of 200 V. Pd particles can be evaporated by the pulse arc plasma gun over the target area whose diameter is 100 mm under the condition of the distance between Pd electrode and the target of 160 mm. This study set the difference between Pd electrode and TiO_2 film at 150 mm, resulting that we can evaporate Pd particle over TiO_2 film uniformly. This study controlled the quantity of loaded Pd by pulse number. This study set the pulse number at 100. According to STEM analysis, the thickness of loaded Pd after 100 pulsation is approximately 60 nm. It is confirmed the Pd/TiO_2 film prepared in this way could not be removed from the netlike glass fiber by rubbing.

2.2. Procedure to characterize Pd/TiO_2 film

This study evaluated the structural and crystal characteristics of Pd/TiO_2 film by SEM (JXA-8530F, produced by JEOL Ltd.), EPMA (JXA-8530F, produced by JEOL Ltd.), STEM (JEM-ARM200F, produced by JEOL Ltd.), EDS (JEM-ARM200F, produced by JEOL Ltd.) and EELS (JEM-ARM2007 Cold, produced by JEOL Ltd.). Electron is used for analysis by these measuring instruments. Therefore, the sample must conduct electron. However, the netlike glass disc cannot conduct electron. Therefore, this study coated carbon on Pd/TiO_2 whose thickness was approximately 15 nm by the dedicated device (JEC-1600, produced by JEOL Ltd.) before analysis.

The electron was emitted on the sample by the electron probe applying the acceleration voltage of 15 kV and the current of 3.0×10^{-8} A to analyze the surface structure of sample by SEM. Simultaneously, EPMA detects the characteristic X-ray. After that, we measured the concentration of chemical element referring to the relation between the characteristic X-ray energy and the atomic

number. The space resolution for SEM and EPMA is 10 μm. We can understand the coating state of prepared photocatalyst as well as measure the quantity of doped metal within TiO_2 film by EPMA analysis.

The electron probe emits electrons to the sample at the acceleration voltage of 200 kV, when the inner structure of the sample is analyzed by STEM. The size, thickness and structure of loaded Pu were evaluated. The X-ray characteristics of the sample is detected by EDS at the same time, so the concentration distribution of chemical element toward thickness direction of the sample is known. In the present paper, the concentration distribution of Ti, Pd and Si were analyzed.

EELS is used to detect elements as well as to determine oxidation states of transition metals. The EELS characterization was determined by JEM-ARM200F equipped with GIF Quantum having 2048 ch. The dispersion of 0.5 eV/ch for the full width at half maximum of the zero loss peak was achieved in the study.

2.3. CO_2 reduction experiment

Figure 1 shows that experimental set-up of the reactor composing of stainless tube (height of 100 mm and inside diameter of 50 mm), Pd/TiO_2 film coated on netlike glass disc (diameter of 50 mm and thickness of 1 mm) located on the teflon cylinder (height of 50 mm and diameter of 50 mm), a quartz glass disc (diameter of 84 mm and thickness of 10 mm), a sharp cut filter cutting off the light whose wavelength is below 400 nm (SCF – 49.5C-42L, produced by SIGMA KOKI CO. LTD.), a 150 W Xe lamp (L2175, produced by Hamamatsu Photonics K. K.), mass flow controller, gas cylinder of CO_2 and H_2.

The volume of reactor to charge CO_2 is 1.25×10^{-4} m^3. The light of Xe lamp which is located inside the stainless tube illuminates Pd/TiO_2 film coated on the netlike glass disc through the sharp cut filter and the quartz glass disc that are at the top of the stainless tube. The wavelength of light illuminating by Xe lamp is distributed from 185 nm to 2000 nm. Since a sharp cut filter can remove UV components of the light from the Xe lamp, the wavelength from Xe lamp is distributed from 401 to 2000 nm with the filter. Figure 2 displays the performance of the sharp cut filter to cut off the wavelength of light, which can prove to remove the light whose wavelength is below 400 nm. The average light intensities of Xe lamp without and with the sharp cut filter are 62.4 mW/cm^2 and 40.6 mW/cm^2, respectively.

CO_2 gas and H_2 gas whose purity were 99.995 vol% and 99.99999 vol%, respectively were controlled by mass flow controller and mixed in the buffer chamber for the CO_2 reduction experiment. After that, they were introduced into the pre-vacuumed reactor using a vacuum pump. We confirmed the mixing ratio of CO_2 and H_2 by TCD gas chromatogragh (Micro GC CP4900, produced by GL Science) before introducing into the reactor. After confirming the mixing ratio of CO_2 and H_2, we injected the distilled water into the reactor via gas sampling tap and started to illuminate Xe lamp together. The injected water was changed into a vapor by the heat of Xe lamp completely. The moral ratio of $CO_2/H_2/H_2O$ was set at 1:0.5:0.5, 1:0.5:1, 1:1:0.5, 1:1:1, 1:2:2. The temperature in reactor rose up to 343 K within one hour and was kept at about 343 K during the experiment due to the heat of Xe lamp.

In CO_2 reduction experiment, we sampled the gas in the reactor every 24 hours. We analyzed the gas samples using FID gas chromatograph (GC353B, produced by GL Science) and methanizer (MT221, produced by GD Science). FID gas chromatograph and methanizer can analyze in the

minimum range of 1 ppmV.

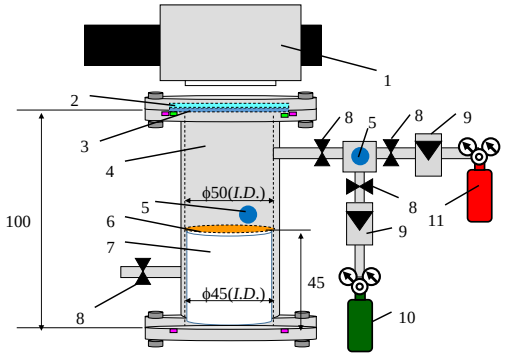

1. Xe lamp, 2. Sharp cut filter, 3. Quartz glass disc, 4. Stainless pipe,
5. Gas sampling tap, 6. Photocatalyst, 7. Teflon cylinder, 8. Valve,
9. Mass flow controller, 10. CO_2 gas cylinder (99.995 vol%),
11. H_2 gas cylinder (99.99999 vol%)

Figure 1. Experimental apparatus for CO_2 reduction [35,36].

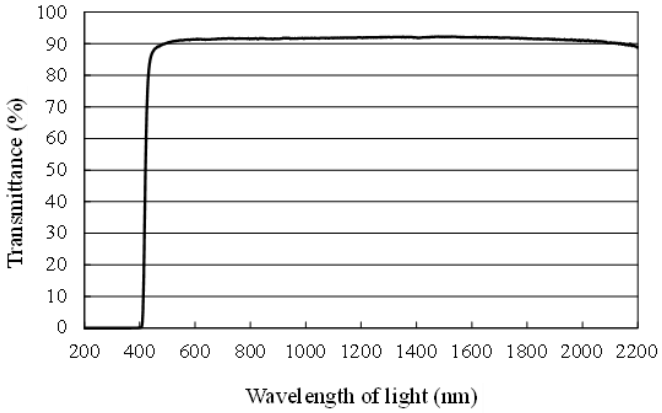

Figure 2. Performance of sharp cut filter to cut off the wavelength of light under 400 nm [35,36].

3. Results and discussion

3.1. Characterization of Pd/TiO₂ film

Figures 3 and 4 show EPMA results of TiO_2 and Pd/TiO_2 film coated on netlike glass disc, respectively. We used 1500 times magnification SEM image for EPMA. In these figures, the different colors identify the concentrations of each element in observation area. For example, light colors such as white, pink, and red display the quantity of element is large. On the other hand, dark colors such as black and blue display the quantity of element is small.

According to Figures 3 and 4, it is obvious that TiO_2 film was coated on netlike glass fiber. Since the thermal conductivity is different between Ti and SiO_2, which are 19.4 W/(m·K) and 1.82 W/(m·K), respectively at 600 K [37], the temperature distribution of TiO_2 solution adhered on the netlike glass disc was not uniform during firing process. It can be considered that crack was formed on the TiO_2 film by the thermal expansion and shrinkage around netlike glass fiber.

In addition, we can observe the uniform loading of nanosized Pd particles on TiO_2 according to Figure 4.

The observation area of diameter of 300 μm which is the center of netlike glass disc is analyzed by EPMA to evaluate the quantity of loaded Pd within TiO_2 film quantitatively. We estimate the ratio of Pd to Ti by averaging the data obtained. As a result, the weight percentages of Pd and Ti in Pd/TiO_2 film are 0.44 wt% and 99.56 wt%, respectively.

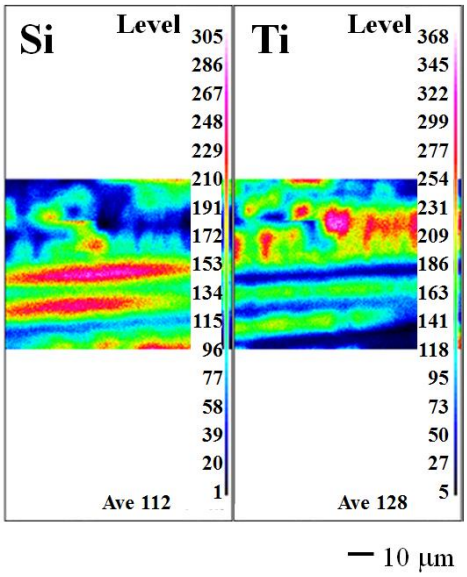

Figure 3. EPMA result of TiO_2 film coated on netlike glass disc.

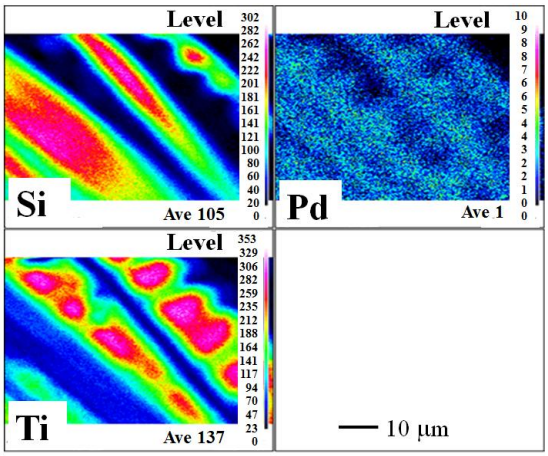

Figure 4. EPMA result of Pd/TiO_2 film coated on netlike glass disc.

Figure 5 shows STEM and EDS results of Pd/TiO_2 film coated on netlike glass disc. 250000 times magnification STEM image was used in the EDS. It is observed that Pd is coated on TiO_2 film according to STEM image, which is confirmed from EDS image. It is also observed that the layers of Pd and Ti are separated. The thickness of the Pd coated is approximately 60 nm. Since the observation area is small compared to EPMA image shown in Figure 4, nano-sized Pd particle is loaded on TiO_2 dispersedly.

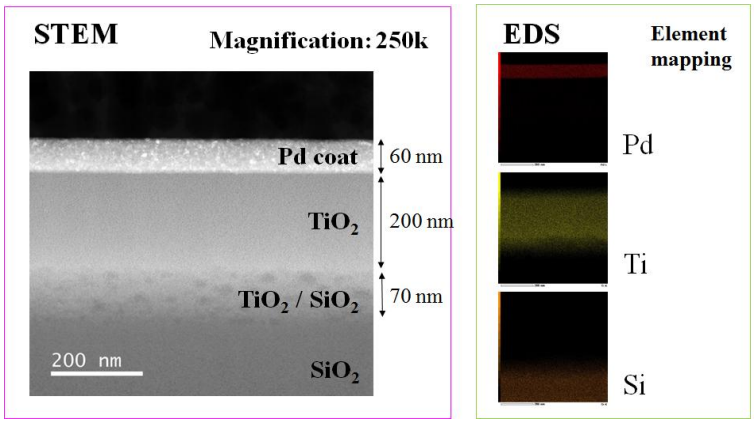

Figure 5. STEM and EDS result of Pd/TiO_2 film coated on netlike glass disc.

Figure 6 shows EELS spectra of Pd in Pd/TiO_2 film in which peaks at around 540 eV can be observed. Compared to the spectra peaks of Pd nanowire, Pd metal and PdO in [38], the EELS spectra of Pd metal matches that in Figure 6. Therefore, it is believed that Pd in Pd/TiO_2 prepared in this study exists as Pd metal. Since the photoreduction performance of Pd/TiO_2 was higher than that of PdO/TiO_2 [25,39], the desirable Pd/TiO_2 without oxidization was proved to be prepared in this study.

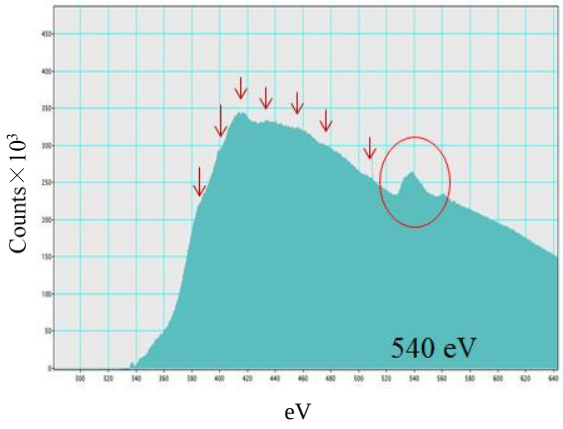

Figure 6. EELS spectra of Pd in Pd/TiO_2.

3.2. Impact of mixing ratio of CO_2, H_2 and H_2O on CO_2 reduction characteristics of Pd/TiO_2

Figures 7 and 8 show the change in concentrations of formed CO and CH_4 with single Pd/TiO_2 film coated on netlike glass disc and overlapped Pd/TiO_2 films with the time under the condition of Xe lamp illumination with UV light, respectively. The error bars in three experiments are also shown in Figures 7 and 8 to demonstrate the reproducibility of prepared Pd/TiO_2, respectively. The amount of Pd/TiO_2 for single film and two films are 0.05 g and 0.18 g, respectively. In this experiment, a blank test conducting the same experiment without Xe lamp illumination had been carried out as a reference, resulting that no fuel was detected as expected. Tables 1 and 2 list maximum concentration of formed CO and CH_4 under the condition shown in Figures 7 and 8, respectively.

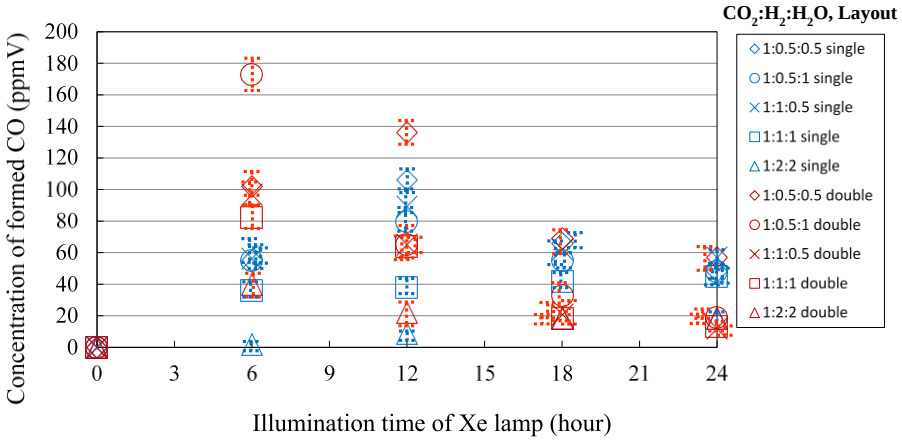

Figure 7. Change in concentration of formed CO with the illumination time among different moral ratios of $CO_2/H_2/H_2O$ with UV light illumination.

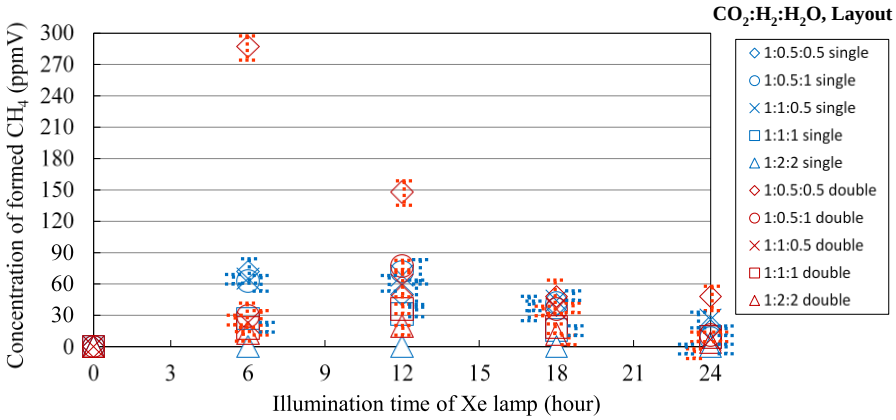

Figure 8. Change in concentration of formed CH_4 with the illumination time among different moral ratios of $CO_2/H_2/H_2O$ with UV light illumination.

Table 1. Comparison of maximum concentration of formed CO with the illumination time among different moral ratios of $CO_2/H_2/H_2O$ with UV light illumination.

	1:0.5:0.5	1:0.5:1	1:1:0.5	1:1:1	1:2:2
Single	106 ppmV	80 ppmV	89 ppmV	45 ppmV	18 ppmV
Double	136 ppmV	173 ppmV	97 ppmV	82 ppmV	40 ppmV

Table 2. Comparison of maximum concentration of formed CH_4 with the illumination time among different moral ratios of $CO_2/H_2/H_2O$ with UV light illumination.

	1:0.5:0.5	1:0.5:1	1:1:0.5	1:1:1	1:2:2
Single	72 ppmV	72 ppmV	68 ppmV	31 ppmV	0 ppmV
Double	287 ppmV	77 ppmV	59 ppmV	36 ppmV	20 ppmV

Figures 7 and 8 reveal that the concentrations of CO and CH_4 for overlapped Pd/TiO_2 discs are

higher than those for single Pd/TiO_2 disc under every moral ratio of $CO_2/H_2/H_2O$. The reasons are believed to be that: (i) The amount of photocatalyst used for photocatalysis reaction is increased. (ii) The electron transfer between two Pd/TiO_2 films promotes the activity of photocatalysis reaction. (iii) The lower positioned Pd/TiO_2 disc utilizes the light passing through the top disc [36].

According to Figure 7 and Table 1, the CO_2 reduction performance to produce CO is the highest at the moral ratio of $CO_2/H_2/H_2O$ = 1:0.5:1 with overlapped Pd/TiO_2 coated netlike glass discs, of which the concentration of CO is 173 ppmV. On the other hand, according to Figure 8 and Table 2, the CO_2 reduction performance to produce CH_4 is the highest for the moral ratio of $CO_2/H_2/H_2O$ = 1:0.5:0.5 with overlapped Pd/TiO_2 films coated netlike glass discs, of which the concentration of CH_4 is 287 ppmV. Since the reaction scheme of $CO_2/H_2/H_2O$ is not fully understood, this study refers to the reaction mechanism of CO_2 with H_2O or H_2 as shown by Eqs 1–11. It is known from the reaction mechanism that the theoretical moral ratio of CO_2 with H_2O or H_2 to produce CO is 1:1. On the other hand, the theoretical moral ratio of with H_2O or H_2 to produce CH_4 is 1:4. The moral ratio of $CO_2/H_2/H_2O$ = 1:0.5:0.5 can be identified with the moral ratio of CO_2/total reductants = 1:1. According to Eqs 1–11, CO is produced first compared to CH_4. In addition, it is believed that some CO might be converted into CH_4 according to Eq 5. Producing CH_4 needs four times H^+ and electrons as many as producing CO needs. Since Pd has high reduction performance [23–25], it is thought that the optimum moral ratio of CO_2/total reductants to produce CH_4 in this study was smaller than the theoretical moral ratio required.

The optimum moral ratio to produce CO found in this study is the moral ratio of $CO_2/H_2/H_2O$ = 1:0.5:1 according to Figure 7 and Table 1. In addition, the second best moral ratio to produce CO is the moral ratio of $CO_2/H_2/H_2O$ = 1:0.5:0.5, which is the optimum moral ratio to produce CH_4 according to Figure 8 and Table 2. As described above, it is believed that some CO might be converted into CH_4. It is thought that more CO converts into CH_4 at the moral ratio of $CO_2/H_2/H_2O$ = 1:0.5:0.5. Therefore, the moral ratio of $CO_2/H_2/H_2O$ = 1:0.5:1, which is close to the moral ratio of $CO_2/H_2/H_2O$ = 1:0.5:0.5, becomes the optimum moral ratio to produce CO. Additionally, the moral ratio of $CO_2/H_2/H_2O$ = 1:0.5:1 is superior to that of $CO_2/H_2/H_2O$ = 1:1:0.5 from the viewpoint of CO production though the moral ratio of CO_2/total reductants is the same. Since H_2 has higher reduction performance than H_2O [40], the moral ratio of $CO_2/H_2/H_2O$ = 1:0.5:1, that would have sufficient H_2 to promote the reduction reaction even less H_2, would be more suitable for CO_2 conversion into CO over Pd/TiO_2.

Table 3 lists the selectivity of products under the condition shown in Figures 7 and 8. The selectivity is calculated using the maximum concentration of formed CO and CH_4. It is revealed that the highest selectivity of CH_4 production is obtained for the moral ratio of $CO_2/H_2/H_2O$ = 1:0.5:0.5 with overlapped Pd/TiO_2 films coated netlike glass discs. Therefore, it can be concluded that the optimum moral ratio of $CO_2/H_2/H_2O$ is 1:0.5:0.5.

Figures 9 and 10 show the moral quantities of CO and CH_4 per weight of photocatalyst with the time under the condition of the Xe lamp illumination with UV light, respectively. The moral quantities of CO and CH_4 obtained with single Pd/TiO_2 film and that with overlapped Pd/TiO_2 are shown in Figures 9 and 10. The quantity of Pd/TiO_2 for single disc and two overlapped discs are 0.05 g and 0.18 g, respectively. Since the data of formed CO and CH_4 shown in Figures 9 and 10 are the same data as shown in Figures 7 and 8, respectively, the error bars are omitted in Figures 9 and 10. This study adopts the photocatalytic activity evaluation using moral quantities of product per weight of photocatalyst since this evaluation is popular in recent photocatalyst studies [41–46].

Before this experiment, a blank test conducting the same experiment without Xe lamp illumination had been carried out as a reference, in which no fuel was detected as expected.

Table 3. Comparison of selectivity of products among different moral ratios of $CO_2/H_2/H_2O$ with UV light illumination.

	1:0.5:0.5	1:0.5:1	1:1:0.5	1:1:1	1:2:2
Single (CO)	59.6 %	52.6 %	56.7 %	59.2 %	100 %
Single (CH_4)	40.4 %	47.4 %	43.3 %	40.8 %	0 %
Double (CO)	32.2 %	69.2 %	62.2 %	69.5 %	66.7 %
Double (CH_4)	67.8 %	30.8 %	37.8 %	30.5 %	33.3 %

According to Figures 9 and 10, the moral quantities of CO and CH_4 per weight of photocatalyst in two Pd/TiO_2 discs case overlapped are lower than those for single Pd/TiO_2 disc case except for the moral ratio of $CO_2/H_2/H_2O$ = 1:0.5:0.5. The reason why the moral quantities of CO and CH_4 per weight of photocatalyst in overlapped case are lower than those in single case is considered to be: (i) Some parts of the Pd/TiO_2 film on the lower positioned disc can't receive the light. (ii) If the produced fuel keeps within space between two discs, this prevents CO_2, H_2 and H_2O from contacting the surface of photocatalyst. As a result, the photoreduction cannot progress well [36]. However, in the case of the moral ratio of $CO_2/H_2/H_2O$ is 1:0.5:0.5, the moral quantity of CH_4 per weight of photocatalyst for overlapped case which is 8.14 μmol/g is approximately 1.1 times larger than that for single Pd/TiO_2 disc. On the other hand, the moral quantity of CO per weight of photocatalyst for single Pd/TiO_2 disc which is 10.8 μmol/g is approximately 2.8 times as large as that for overlapped case. Since the high reduction performance is necessary to produce CH_4 via CO as mentioned above, the high CO_2 reduction performance is obtained for the moral ratio of $CO_2/H_2/H_2O$ = 1:0.5:0.5 with two overlapped Pd/TiO_2 discs.

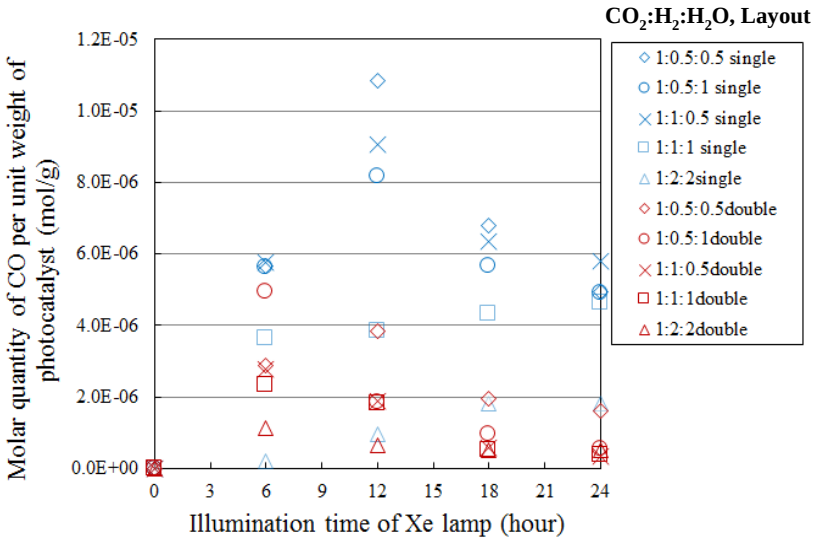

Figure 9. Change in moral quantity of CO per unit weight of photocatalyst with the illumination time among different moral ratios of $CO_2/H_2/H_2O$ with UV light illumination.

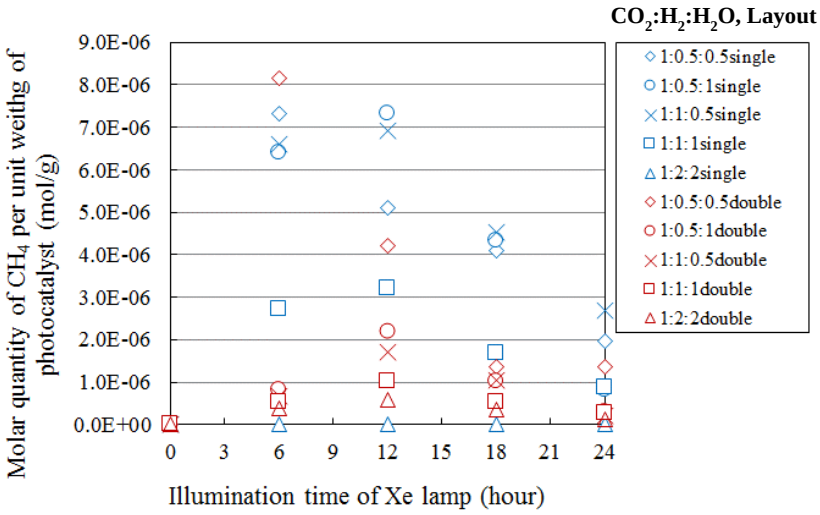

Figure 10. Change in moral quantity of CH_4 per unit weight of photocatalyst with the illumination time among different moral ratios of $CO_2/H_2/H_2O$ with UV light illumination.

Figure 11 shows the change in concentrations of formed CO with the time under the condition of Xe lamp illumination without UV light. CO is only detected as a fuel produced from this experiment. The error bars in three experiments are also shown in Figure 10 to demonstrate the reproducibility of prepared Pd/TiO_2. Before this experiment, a blank test conducting the same experiment without Xe lamp illumination had been carried out as a reference, in which no fuel was detected as expected. In addition, TiO_2 did not display the CO_2 reduction performance under the illumination condition of Xe lamp without UV light. The CO_2 reduction performance has been realized by Pd doping under the illumination condition of Xe lamp without UV light. Table 4 lists maximum concentration of formed CO under the condition shown in Figure 11.

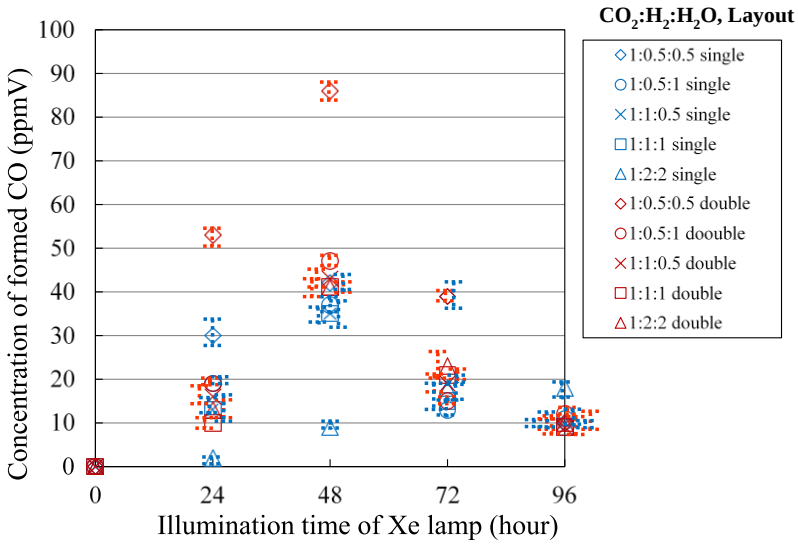

Figure 11. Change in concentration of formed CO with the illumination time among different moral ratios of $CO_2/H_2/H_2O$ without UV light illumination.

Table 4. Comparison of maximum concentration of formed CO among different moral ratios of $CO_2/H_2/H_2O$ without UV light illumination.

	1:0.5:0.5	1:0.5:1	1:1:0.5	1:1:1	1:2:2
Single	42 ppmV	37 ppmV	35 ppmV	35 ppmV	18 ppmV
Double	86 ppmV	47 ppmV	43 ppmV	41 ppmV	41 ppmV

Figure 11 reveals that the concentrations of CO with two overlapped Pd/TiO_2 discs are higher than those with single Pd/TiO_2 disc under every moral ratio of $CO_2/H_2/H_2O$. The same reason of this result as UV light illumination case can be considered. In addition, the CO_2 reduction performance is the highest for the moral ratio of $CO_2/H_2/H_2O$ = 1:0.5:0.5 in this case, where the concentration of CO is 86 ppmV as shown in Table 4. Therefore, it can be concluded that the optimum moral ratio of $CO_2/H_2/H_2O$ is 1:0.5:0.5. It is considered that the same reaction mechanism as mentioned in the UV light illumination case is conducted. The CO_2 reduction performance of Pd/TiO_2 under the condition of Xe lamp illumination without UV light is lower than that under the condition of Xe lamp illumination with UV light. Therefore, it is revealed that Pd/TiO_2 obtains the main photoenergy from UV light.

Figure 12 shows the moral quantity of CO per weight of photocatalyst with the time under the condition of Xe lamp illumination without UV light. Since the data of formed CO shown in Figure 12 are the same data as shown in Figures 11, the error bars are omitted in Figure 12. Similarly, before this experiment, a blank test conducting the same experiment without Xe lamp illumination had also been carried out as a reference, in which no fuel was detected as expected. Since TiO_2 did not display the CO_2 reduction performance under the illumination condition of Xe lamp without UV light. The CO_2 reduction performance has been realized by Pd doping under the illumination condition of Xe lamp without UV light. It is seen that the moral quantities of CO per weight of photocatalyst with overlapped discs are lower than those with the single Pd/TiO_2 disc under every moral ratio of $CO_2/H_2/H_2O$. The highest moral quantity of CO per weight of photocatalyst in overlapped case is obtained under the moral ratio of $CO_2/H_2/H_2O$ is 1:0.5:0.5, which is 3.97 μmol/g. This is 59% of moral quantity of CO per weight of photocatalyst in single disc case. The same reasons explained in the case of illumination with UV light are thought to cause this result as well. Figure 13 displays the image of mass and electron transfer between overlapped photocatalyst discs to explain that produced fuel of CO would block the reactants of CO_2, H_2 and H_2O to contact the surface of photocatalyst. This figure illustrates the reason for lower performance of two overlapped discs case.

In this study, the highest moral quantity of CH_4 per weight of photocatalyst is 8.14 μmol/g in overlapped discs case under the condition of Xe lamp illumination with UV light. The previous studies reported the moral quantities of CH_4 per weight of photocatalyst in the case of CO_2/H_2O with Pd/TiO_2 were 25, 4.8 and 1.9 μmol/g [23–25]. The other study reported that the moral quantities of CH_4 per weight of photocatalyst in the case of CO_2/H_2 with Pd/TiO_2 was 356 μmol/g [26].

However, the highest moral quantity of CO per weight of photocatalyst is 10.8 μmol/g in single disc case under the condition of Xe lamp illumination with UV light in this study. The previous studies reported that the moral quantities of CO per weight of photocatalyst in the case of CO_2/H_2O with Pd/TiO_2 were 0.12 and 0.13 μmol/g [14,15]. The other study reported that the moral quantity of CO per weight of photocatalyst in the case of CO_2/H_2 with Pd/TiO_2 was 45 μmol/g [26].

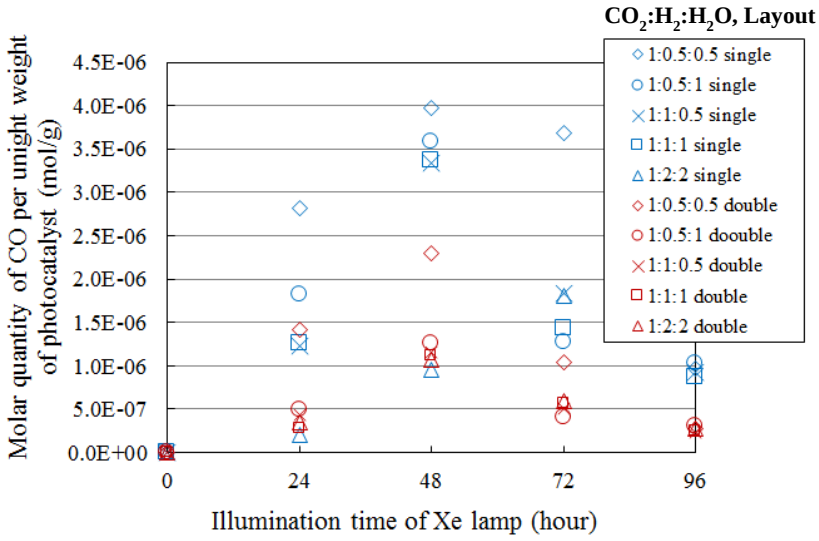

Figure 12. Change in moral quantity of CO per unit weight of photocatalyst with the illumination time among several moral ratios of $CO_2/H_2/H_2O$ without UV light illumination.

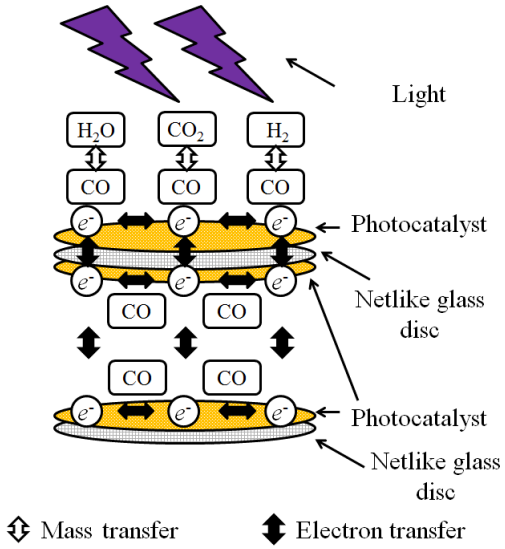

Figure 13. Image of mass and electron transfer in the case of overlapped Pd/TiO_2.

This study also investigates the quantum efficiency which is well known as a factor to evaluate the photocatalytic activity and efficiency [47]. The quantum efficiency is calculated by the following equation [48]:

$$\eta = (N_{output}/N_{input}) \times 100 \quad (12)$$

$$N_{input} = (I \times t \times \lambda \times A_{re})/(h \times c) \quad (13)$$

$$N_{output} = N_{CO}M_{CO}N_A + N_{CH4}M_{CH4}N_A \quad (14)$$

where η is the quantum efficiency (%), N_{input} is the number of photon absorbed by photocatalyst (-),

N_{output} is the number of photon used for photocatalytic reaction (-), I is the light intensity of UV light (W/cm^2), t is the UV light illumination time (s), λ is the wave length limit of light which photocatalyst absorbs for photocatalytic reaction (m), A_{re} is the reaction surface area of photocatalyst which is assumed to be equal to one surface area of netlike glass disc (cm^2), h is Plank's constant (=6.626 × 10^{-34}) (J s), c is light speed (=2.998 × 10^8) (m/s), N_{CO} is the electron number which is necessary for forming CO of a molecular (=2) (-), M_{CO} is the moral number of formed CO (mol), N_A is Avogadro's number (=6.022 × 10^{23}) (1/mol), N_{CH4} is the electron number which is necessary for forming CH_4 of a molecular (-), M_{CH4} is the moral number of formed CH_4 (=8) (mol). In this study, I averaged during all experiments under the condition of Xe lamp illumination with UV light and without UV light were 62.4 mW/cm^2 and 40.6 mW/cm^2, respectively. t under the condition of Xe lamp illumination with UV light and without UV light were 86400 s (=24 hours) and 345600 s (=96 hours).

Figures 14 and 15 show the quantum efficiency among different moral ratios of $CO_2/H_2/H_2O$ under the condition of Xe lamp illumination with and without UV light, respectively. They revealed that the highest quantum efficiency is obtained at the moral ratio of $CO_2/H_2/H_2O$ = 1:0.5:0.5 with two overlapped Pd/TiO_2 discs under the condition of Xe lamp illumination not only with UV light but also without UV light, which follows the results shown in Figures 8 and 11. The highest quantum efficiency under the condition of Xe lamp illumination with UV light is 3.21 × 10^{-3}%, while that under the condition of Xe lamp illumination without UV light is 7.99 × 10^{-5}%.

According to the comparison with the previous studies in the case of CO_2/H_2O or CO_2/H_2 mentioned above, the CO and CH_4 production performance achieved in this study is higher than that reported in the case of CO_2/H_2O [23–25], while it is lower than that reported in the case of CO_2/H_2 [26]. Though it is thought that the doped Pd can provide the free electron not only to prevent the recombination of electron and hole produced but also to improve the light absorption effect, it was not confirmed that the CO_2 reduction performance was improved significantly in this study.

This study suggests that different metals should be doped on the higher and the lower positioned photocatalysts discs to promote the CO_2 reduction performance more. The co-doped TiO_2 such as PbS–Cu/TiO_2, Cu–Fe/TiO_2, Cu–Ce/TiO_2, Cu–Mn/TiO_2 and Cu–CdS/TiO_2 was reported to promote the CO_2 reduction performance of TiO_2 with H_2O [4,40]. Then, the promotion of CO_2 reduction performance by different metal doping is expected when the combination of $CO_2/H_2/H_2O$ is considered. Furthermore, the dopant such as Fe absorbing the shorter wavelength light than Pd [49] can be suggested to be used at the higher located layer. The wavelength of light extends after penetrating the higher located photocatalyst [50]. Therefore, the overlapping of the higher positioned Fe/TiO_2 which absorbs the shorter wavelength light and the lower positioned Pd/TiO_2 which absorbs the longer wavelength light may be an effective way for utilization of wide range light. This proposal is almost the same as the idea of hybridizing two photocatalysts which have different band gaps [10,51–53].

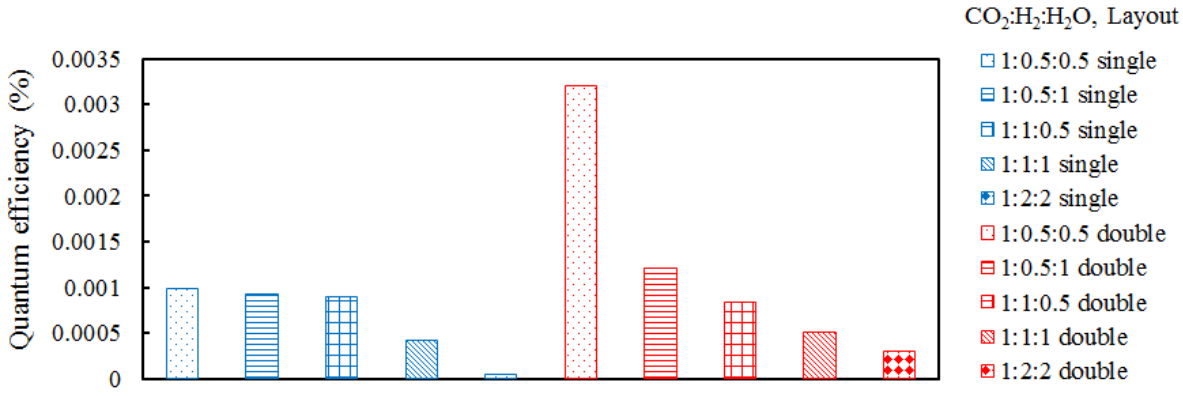

Figure 14. Comparison of quantum efficiency among different moral ratios of $CO_2/H_2/H_2O$ with UV light illumination.

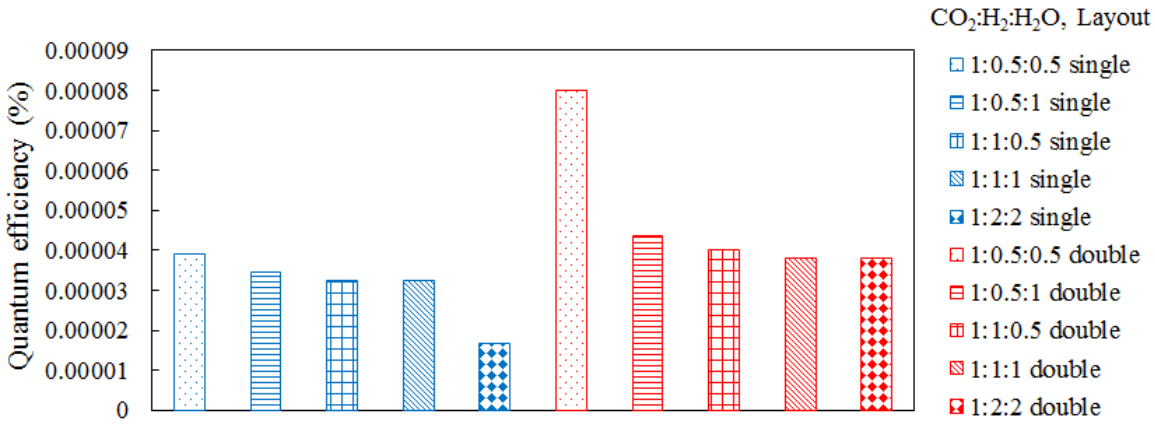

Figure 15. Comparison of quantum efficiency among different moral ratios of $CO_2/H_2/H_2O$ without UV light illumination.

4. Conclusions

This study obtained the following conclusions based on the investigation:

The nanosized Pd particles could be loaded on TiO_2 uniformly by pulse arc plasma method. Pd in Pd/TiO_2 prepared by this method exists in the form of Pd metal.

With UV light, the concentrations of CO and CH_4 with two overlapped Pd/TiO_2 discs are higher than those with single Pd/TiO_2 disc under every moral ratio of $CO_2/H_2/H_2O$. The CO_2 reduction performance for producing CO is the highest at the moral ratio of $CO_2/H_2/H_2O$ = 1:0.5:1 with two overlapped Pd/TiO_2 films coated on netlike glass discs, where the concentration of CO is 173 ppmV. The CO_2 reduction performance to produce CH_4 is the highest at the moral ratio of $CO_2/H_2/H_2O$ = 1:0.5:0.5 with two overlapped Pd/TiO_2 films coated on netlike glass discs, where the concentration of CH_4 is 287 ppmV. In addition, the moral quantities of CO and CH_4 per weight of photocatalyst in two overlapped Pd/TiO_2 discs case are lower than those for single Pd/TiO_2 disc case except at the moral ratio of $CO_2/H_2/H_2O$ = 1:0.5:0.5. When the moral ratio of $CO_2/H_2/H_2O$ is 1:0.5:0.5, the moral quantity of CH_4 per weight of photocatalyst with two overlapped Pd/TiO_2 discs which is 8.14 μmol/g

is about 1.1 times larger than that with single Pd/TiO_2 disc. It can be concluded that the optimum moral ratio of CO_2/H_2/H_2O is 1:0.5:0.5.

Without UV light, the concentrations of CO with two overlapped Pd/TiO_2 discs are also higher than those with single Pd/TiO_2 disc under every moral ratio of CO_2/H_2/H_2O. The CO_2 reduction performance is the highest at the moral ratio of CO_2/H_2/H_2O = 1:0.5:0.5, where the concentration of CO is 86 ppmV. Therefore, it can be concluded that the optimum moral ratio of CO_2/H_2/H_2O is 1:0.5:0.5. In addition, the moral quantities of CO per weight of photocatalyst in two discs case are lower than those in single Pd/TiO_2 disc case under every moral ratio of CO_2/H_2/H_2O. The highest moral quantity of CO per weight of photocatalyst in two discs overlapped case is obtained under the moral ratio of CO_2/H_2/H_2O is 1:0.5:0.5, which is 3.97 μmol/g. This is 59% of moral quantity of CO per weight of photocatalyst in single disc case.

Acknowledgments

The authors appreciate for not only JSPS KAKENHI Grant Number 16K06970 but also joint research program of the Institute of Materials and Systems for Sustainability, Nagoya University for the economic assistance.

Conflict of interest

The authors declare that this paper has no conflict of interest for the publication.

References

1. Greenhouse Gases Observing Satellite GOSAT "IBUSUKI", 2019. Available from: http://www.gosat.nies.go.jp/en/.
2. Tahir M, Amin NS (2015) Indium-doped TiO_2 nanoparticles for photocatalytic CO_2 reduction with H_2O vapors to CH_4. *Appl Catal B-Environ* 162: 98–109.
3. Abdulah H, Khan MMR, Ong HR, et al. (2017) Modified TiO_2 photocatalyst for CO_2 photocatalytic reduction: an overview. *J CO_2 Util* 22: 15–32.
4. Sohn Y, Huang W, Taghipour F (2017) Recent progress and perspectives in the photocatalytic CO_2 reduction of Ti-oxide-based nanomaterials. *Appl Surf Sci* 396: 1696–1711.
5. Nahar S, Zain MF, Kadhum AAH, et al. (2017) Advances in photocatalytic CO_2 reduction with water: A Review. *Materials* 10: 629.
6. Ola O, Maroto-Valer MM (2015) Review of material design and reactor engineering on TiO_2 photocatalysis for CO_2 reduction. *J Photoch Photobio C* 24: 16–42.
7. Xie S, Wang Y, Zhang Q, et al. (2014) MgO- and Pt-promoted TiO_2 as an efficient photocatalyst for the prefential reduction of carbon dioxide in the presence of water. *ACS Catal* 4: 3644–3653.
8. Khalid NR, Ahmed E, Niaz NA, et al. (2017) Highly visible light responsive metal loaded N/TiO_2 nanoparticles for photocatalytic conversion of CO_2 into methane. *Ceram Int* 43: 6771–6777.
9. Tan LL, Ong WJ, Chai SP, et al. (2015) Noble metal modified reduced graphene oxide/TiO_2 ternary nanostructures for efficient visible-light-driven photoreduction of carbon dioxide into methane. *Appl Catal B-Environ* 166–167: 251–259.

10. Cmarillo R, Toston S, Martinez F, et al. (2018) Improving the photo-reduction of CO_2 to fuels with catalysts synthesized under high pressure: Cu/TiO_2. *J Chem Technol Biot* 93: 1237–1248.
11. Aguirre ME, Zhou R, Eugene AJ, et al. (2017) Cu_2O/TiO_2 heterostructures for CO_2 reduction through a direct z-scheme: protecting Cu_2O from photocorrosion. *Appl Catal B-Environ* 217: 485–493.
12. Marci G, Garcia-Lopez EI, Palmisano L (2014) Photocatalytic CO_2 reduction in gas-solid regime in the presence of H_2O by using GaP/TiO_2 composite as photocatalyst under simulated solar light. *Catal Commun* 53: 38–41.
13. Beigi AA, Fatemi S, Salehi Z (2014) Synthesis of nanocomposite CdS/TiO_2 and investigation of its photocatalytic activity of CO_2 reduction to CO and CH_4 under visible light irradiation. *J CO_2 Util* 7: 23–29.
14. Fang Z, Li S, Gong Y, et al. (2014) Comparison of catalytic activity of carbon-based AgBr nanocomposites for conversion of CO_2 under visible light. *J Saudi Chem Soc* 18: 299–307.
15. Xu F, Zhang J, Zhu B, et al. (2018) $CuInS_2$ sensitized TiO_2 hybrid nanofibers for improved photocatalytic CO_2 reduction. *Appl Catal B-Environ* 230: 194–202.
16. Camarillo R, Toston S, Martinez F, et al. (2017) Preparation of TiO_2-based catalysts with supercritical fluid technology: characterization and photocatalytic activity in CO_2 reduction. *J Chem Technol Biot* 92: 1710–1720.
17. Wei Y, Jiao J, Zhao Z, et al. (2015) 3D ordered macroporous TiO_2-supported Pt@CdS core-shell nanoparticles: design, synthesis and efficient photocatalytic conversion of CO_2 with water to methane. *J Mater Chem A* 20: 11074–11085.
18. Zhao Y, Wei Y, Wu X, et al. (2018) Graphene-wrapped Pt/TiO_2 photocatalysts with enhanced photogenerated charges separation and reactant adsorption for high selective photoreduction of CO_2 to CH_4. *Appl Catal B-Environ* 226: 360–372.
19. Toston S, Camarillo R, Martinez F, et al. (2017) Supercritical synthesis of platinum-modified titanium dioxide for solar fuel production from carbon dioxide. *Chinese J Catal* 38: 636–650.
20. Jiao J, Wei Y, Zhao Y, et al. (2017) AuPd/3DOM-TiO_2 catalysts for photocatalyic reduction of CO_2: high efficient separation of photogenerated charge carriers. *Appl Catal B-Environ* 209: 228–239.
21. Camrillo R, Toston S, Martinez F, et al. (2017) Enhancing the photocatalytic reduction of CO_2 through engineering of catalysts with high pressure technology: Pd/TiO_2 photocatalysts. *J Supercrit Fluid* 123: 18–27.
22. Chen W, Wang Y, Shangguan W (2019) Metal (oxide) modified (M = Pd, Ag, Au and Cu) $H_2SrTa_2O_7$ for photocatalytic CO_2 reduction with H_2O: the effect of cocatalysts on promoting activity toward CO and H_2 evolution. *Int J Hydrogen Energ* 44: 4123–4132.
23. Yu Y, Lan Z, Guo L, et al. (2018) Synergistic effects of Zn and Pd species in TiO_2 towards efficient photo-reduction of CO_2 into CH_4. *New J Chem* 42: 483–488.
24. Singhal N, Kumar U (2017) Noble metal modified TiO_2: selective photoreduction of CO_2 to hydrocarbons. *Mol Catal* 439: 91–99.
25. Yui T, Kan A, Saitoh C, et al. (2011) Photochemical reduction of CO_2 using TiO_2: effects of organic adsorbates on TiO_2 and deposition of Pd onto TiO_2. *ACS Appl Mater Inter* 3: 2594–2600.

26. Li N, Liu M, Yang B, et al. (2017) Enhanced photocatalytic performance toward CO_2 hydrogenation over nanosized TiO_2-loaded Pd under UV irradiation. *J Phys Chem* 121: 2923–2932.
27. Goren Z, Willner I, Nelson AJ, et al. (1990) Selective photoreduction of CO_2/HCO_3^- to formate by aqueous suspensions and colloids of Pd-TiO_2. *J Phys Chem* 94: 3784–3790.
28. Tseng IH, Chang WC, Wu JCS (2002) Photoreduction of CO_2 using sol-gel derived titania and titania-supported copper catalysts. *Appl Catal B-Environ* 37: 37–38.
29. Nishimura A, Sugiura N, Fujita M, et al. (2007) Influence of preparation conditions of coated TiO_2 film on CO_2 reforming performance. *Kagaku Kogaku Ronbun* 33: 146–153.
30. Izumi Y (2013) Recent advances in the photocatalytic conversion of carbon dioxide to fuels with water and/or hydrogen using solar energy and beyond. *Coordin Chem Rev* 257: 171–186.
31. Lo CC, Hung CH, Yuan CS, et al. (2007) Photoreduction of carbon dioxide with H_2 and H_2O over TiO_2 and ZrO_2 in a circulated photocatalytic reactor. *Sol Energ Mat Sol C* 91: 1765–1774.
32. Mahmodi G, Sharifnia S, Madani M, et al. (2013) Photoreduction of carbon dioxide in the presence of H_2, H_2O and CH_4 over TiO_2 and ZnO photocatalysts. *Sol Energy* 97: 186–194.
33. Jensen J, Mikkelsen M, Krebs FC (2011) Flexible substrates as basis for photocatalytic reduction of carbon dioxide. *Sol Energ Mat Sol C* 95: 2949–2958.
34. Nishimura A, Ishida N, Tatematsu D, et al. (2017) Effect of Fe loading condition and reductants on CO_2 reduction performance with Fe/TiO_2 photocatalyst. *Int J Photoenergy* 2017: 1625274.
35. Nishimura A, Tatematsu D, Toyoda R, et al. (2019) Effect of Overlapping Layout of Fe/TiO_2 on CO_2 Reduction with H_2 and H_2O. *MOJ Sol Photoenergy Syst* 3: 1–8.
36. Nishimura A, Toyoda R, Tatematsu D, et al. (2018) Effect of Molar Ratio of H_2 and H_2O on CO_2 Reduction Characteristics of Overlapped Cu/TiO_2. *Int J Eng Sci Invent* 7: 18–28.
37. Japan Society of Mechanical Engineering (1993) *Heat Transfer Hand Book*, 1 Eds, Tokyo: Maruzen.
38. Wang D, Zhou WL, McCaughy BF, et al. (2003) Electrodeposition of metallic nanowire thin films using mesoporous silica templates. *Adv Mater* 15: 130–133.
39. Koci K, Matejova L, Reli M, et al. (2014) Sol-gel derived Pd supported TiO_2-ZrO_2 and TiO_2 photocatalysts; their examination in photocatalytic reduction of carbon dioxide. *Catal Today* 230: 20–26.
40. Wei Y, Wu X, Zhao Y, et al. (2018) Efficient photocatalysts of TiO_2 nanocrystals-supported PtRu alloy nanoparticles for CO_2 reduction with H_2O: synergistic effect of Pt-Ru. *Appl Catal B-Environ* 236: 445–457.
41. Zhang R, Huang Z, Li C, et al. (2019) Monolithic g-C_3N_4/reduced graphene oxide aerogel with in situ embedding of Pd nanoparticles for hydrogenation of CO_2 to CH_4. *Appl Surf Sci* 475: 953–960.
42. Kulandaivalu T, Rashid SA, Sabli N, et al. (2019) Visible light assisted photocatalytic reduction of CO_2 to ethane using CQDs/Cu_2O nanocomposite photocatalyst. *Diam Relat Mater* 91: 64–73.
43. Zhu Z, Huang WR, Chen CY, et al. (2018) Preparation of Pd-Au/TiO_2-WO_3 to enhance photoreduction of CO_2 to CH_4 and CO. *J CO_2 Util* 28: 247–254.
44. Tasbihi M, Fresno F, Simon U, et al. (2018) On the selectivity of CO_2 photoreduction towards CH_4 using Pt/TiO_2 catalysts supported on mesoporous silica. *Appl Catal B-Environ* 239: 68–76.

45. Wei Y, Wu X, Zhao Y, et al. (2018) Efficient photocatalysts of TiO_2 nanocrystals-supported PtRu alloy nanoparticles for CO_2 reduction with H_2O: synergistic effect of Pt-Ru. *Appl Catal B-Environ* 236: 445–457.
46. Hashemizadeh I, Golovko VB, Choi J, et al. (2018) Photocatalytc reduction of CO_2 to hydrocarbons using bio-templated porous TiO_2 architectures under UV and visible light. *Chem Eng J* 347: 64–73.
47. Hoque MA, Guzman MJ (2018) Photocatalytic activity: experimental features to report in heterogeneous photocatalysis. *Materials* 11: 1990.
48. Nishimura A, Okano Y, Hirota M, et al. (2011) Effect of preparation condition of TiO_2 film and experimental condition on CO_2 reduction performance of TiO_2 photocatalyst membrane reactor. *Int J Photoenergy* 2011: 305650.
49. Tahir M, Amin NS (2013) Advances in visible light responsive titanium oxide-based photocatalysts for CO_2 conversion to hydrocarbon fuels. *Energ Convers Manage* 76: 194–214.
50. Nagaveni K, Hedge MS, Madras G (2004) Structure and photocatalytic activity of $Ti_{1-x}M_xO_{2\pm\delta}$ (M = W, V, Ce, Zr, and Cu) synthesized by solution combustion method. *J Phys Chem B* 108: 20204–20212.
51. Li L, Gao F, Zhao H, et al. (2013) Tailoring Cu valence and oxygen vacancy in Cu/TiO_2 catalysts for enhanced CO_2 photoreduction efficiency. *Appl Catal B-Environ* 134–135: 349–358.
52. Song G, Xin F, Chen J, et al. (2014) Photocatalytic reduction of CO_2 in cyclohexanol on $CdS-TiO_2$ heterostructured photocatalyst. *Appl Catal A-Gen* 473: 90–95.
53. Song G, Xin F, Yin X (2015) Photocatalytic reduction of carbon dioxide over $ZnFe_2O_4/TiO_2$ nanobelts heterostructure in cyclohexanol. *J Colloid Interf Sci* 442: 60–66.

AIMS Press